Surfactant adsorption kinetics by total internal reflection Raman spectroscopy. Part II: CTAB and Triton X-100 mixtures on silica

David A. Woods[1], Jordan Petkov[2], Colin D. Bain[1*]

1. University of Durham, Department of Chemistry, University Science Laboratories, South Road, Durham, UK, DH1 3LE

2. Unilever Research and Development Laboratory, Port Sunlight, Quarry Road East, Bebington, Wirral, U.K.

Abstract

Total internal reflection (TIR) Raman spectroscopy has been used to study the kinetics of adsorption, desorption and displacement of mixed surfactant systems at the silica-water interface. The limited penetration depth of the evanescent wave provides surface sensitivity while the chemical sensitivity of Raman scattering permits the determination of the time-dependent composition of the adsorbed film. Principal component analysis is used to deconvolute the Raman spectra with a time resolution of 2 s and a precision of 5% of a monolayer. Both equilibrium and kinetic measurements are presented for the cetyltrimethylammonium bromide (CTAB)/Triton X-100 system over a range of concentrations and compositions. For a total concentration of 2 mM, the adsorption isotherm shows strong synergistic behavior with the addition of small amounts of CTAB (~2% of the total surfactant) doubling the adsorbed amount of Triton X-100. This synergism has a marked influence on the kinetics: for example, when Triton X-100 replaces CTAB the Triton X-100 surface excess overshoots its equilibrium value and returns only very slowly to equilibrium. For systems above the cmc, the repartitioning of surfactant between micelles and monomers results in unexpected behavior during exchange or rinsing of mixed surfactant solutions. For example, during rinsing the more rapid diffusion of CTAB away from the surface leads to a local increase in the monomer concentration of Triton X-100 resulting in a temporary spike in the Triton X-100 surface excess. Displacement kinetics of CTAB by TX-100 and vice versa are generally slower than the adsorption or desorption of the pure surfactants, but cover a wide range of kinetic timescales depending on the details of the compositions and concentrations of the initial and final solutions.

Introduction

This paper constitutes the second of a series on the measurement of adsorption kinetics of surfactants at the solid–liquid interface by total internal reflection (TIR) Raman spectroscopy. In Part I, we introduced the technique of TIR-Raman spectroscopy and demonstrated the sensitivity and time resolution achievable. The cationic surfactant cetyltrimethylammonium bromide (CTAB) and the non-ionic surfactant Triton X-100 (TX-100) were used as exemplars. A wall-jet cell provided controlled hydrodynamics and allowed quantitative modelling of the adsorption kinetics. In Part II of this series, we show how TIR Raman spectroscopy can be used to follow the interfacial kinetics of two surfactants in a mixed system. Building on the knowledge from Part I, we use the system CTAB + TX-100. We show that the spectra of binary mixed layers can be decomposed into the two component spectra without the use of selective deuteration and with acquisition times of only 1 second.

While pure surfactants provide important model systems for the study of the thermodynamics and kinetics of adsorption, practical applications of surfactants invariably involve mixtures for several reasons. First, commercial surfactants are not pure compounds but contain a range of chain lengths or degrees of polymerization, unreacted precursors or hydrolysis products. As an example, small amounts of dodecanol present in sodium dodecyl sulfate drastically change the properties of adsorbed films, especially at concentrations below the critical micelle concentration.[1] Second, mixtures of surfactants often produced enhanced performance over the pure components.[2] For example, hand-dishwashing detergents are typically mixtures of three or more surfactants. Third, surfactants may be added to formulations for distinct purposes[3] – as wetting agents, dispersants, detergents, foam stabilizers[4] or friction modifiers.[5] Understanding and controlling the interaction of different surfactants is an essential aid to effective formulation.

Most techniques that can determine the chemical composition of adsorbed surfactant layers are only suitable for equilibrium measurements or the study of slow kinetics on timescales of minutes to hours. Examples are depletion studies, in which a powder is suspended in a surfactant solution and the surfactant remaining in the solution is measured either *in situ* or following removal of an aliquot,[6] and neutron reflection,[7] in which selective deuteration allows surfactants to be distinguished. Conversely, techniques that respond rapidly to sub-monolayer changes in the mass of an adsorbed film – such as reflectometry, surface plasmon resonance or quartz crystal microbalance measurements – lack the chemical selectivity to determine the composition of the adsorbed layer. Where one species is irreversibly adsorbed – as is often the case in polymer-surfactant mixtures – the composition of the mixed layer can be inferred from the rinsing behavior in pure solvent, on the assumption that only the surfactant desorbs. Velegol and Tilton used this approach to study the adsorption of mixtures of CTAB and poly-lysine onto silica[8] while Postmus *et al.* studied the adsorption of polyethylene oxide mixed with a variety of different ethylene oxide alkyl ethers (C_nE_m).[9] For surfactant-surfactant mixtures it is much more difficult to distinguish the two components. Tiberg and coworkers investigated mixtures of different C_nE_m surfactants by optical reflectometry[10] but needed to assume ideal mixing in order to analyze their data quantitatively.

Spectroscopy is a standard way to distinguish chemical species but most common surfactants do not absorb light in the visible or near-UV, nor do they fluoresce, so UV-vis absorption spectroscopy and fluorescence detection are not generally applicable. All surfactants have molecular vibrations but IR absorption cross-sections are typically three orders of magnitude weaker than those for allowed electronic transitions while Raman scattering cross-sections are around 13 orders of magnitude weaker than fluorescence cross-sections. Consequently, vibrational spectroscopy of nanometer-thick

layers of mixed surfactants at interfaces is experimentally challenging. Nevertheless, there are a few cases where attenuated total internal reflection (ATR) IR spectroscopy has been used successfully to monitor adsorption kinetics of mixed surfactant systems. Couzis and Gulari looked at the adsorption of sodium dodecyl sulfate (SDS) and sodium dodecanoate onto Al_2O_3 particles affixed to a germanium ATR crystal.[11] The adsorption processes were slow (hours to days, depending on the solution), probably due to a combination of the large surface area of the particles and the slow exchange of solution (the total volume of the cell was exchanged over the course of an hour). Displacement kinetics were determined from the size of the S=O stretching bands of SDS at 1060 and 1200 cm^{-1} although amounts of the two surfactants could not be established quantitatively. An interesting use of ATR-IR was the study by Clark and Ducker of exchange kinetics in adsorbed films of tetradecyl trimethylammonium bromide (C_{14}TAB) on silica. They replaced a solution of hydrogenated C_{14}TAB with deuterated C_{14}TAB and measured the rate at which the C–H bonds were replaced by C–D bonds.[12] A multiple reflection Si substrate yielded sufficient signal to take a spectrum every two seconds, but also raised the problem of rapidly exchanging the solution in contact with a large substrate. Clark and Ducker solved this problem ingeniously by inserting an air bubble into the cell between the incoming and outgoing solution, which efficiently displaced the initial solution. Li and Tripp studied the replacement of CTAB on TiO_2 particles by deuterated SDS.[13] The exchange process took place over the course of ~1 hr and was followed with a time resolution of ca. 5 minutes per spectrum. Shifts in the frequency of the C–H bands were attributed to changes in the packing of surface aggregates and the relative amounts of the two surfactants were determined by integration of peak areas in the C–H and C–D stretching regions. Tabor *et al.* measured fast surfactant adsorption (~20s) with slower surfactant desorption (~200s) for non-ionic surfactant dissolved in a toluene solution.[14] The use of an organic solvent removed the strong IR water peak, but a multiple bounce ATR crystal was still necessary to obtain sufficient signal. In our own work, we have shown how *external* reflection FTIR spectroscopy can be used to study the adsorption kinetics of surfactant mixtures at the air-water interface without the need for selective deuteration of surfactants.[15] The use of a continually expanding liquid surface allowed measurements at surface ages around 0.1 s.

There are no previous reports of the use of Raman scattering to study the kinetics of adsorption of mixed surfactant systems.

The system we have chosen to study here is a binary mixture of a cationic and non-ionic surfactant. No kinetic studies have been carried out on such mixtures and only a limited amount of work has been published on equilibrium adsorption properties, which we summarize briefly here. Huang and Gu looked at the adsorption of a mixture of CTAB and TX-100 onto a silica gel,[16] finding that for the individual components ~5 times more TX-100 adsorbed than CTAB. TX-100 exhibited a smooth increase to the limiting surface excess while the CTAB showed a plateau in adsorption at both low and high concentration. In the mixed system, adsorption of CTAB was promoted at low total surfactant concentrations; adsorption of both surfactants was inhibited at high total concentrations with the limiting surface excess similar to that of pure CTAB. McDermott *et al.* studied the adsorption of CTAB + $C_{12}E_6$ on quartz by neutron reflection.[17] The CTAB/$C_{12}E_6$ system is chemically similar to CTAB/TX-100 although the cmc of $C_{12}E_6$, and hence of the mixed systems, is much lower than for TX-100. They found that small amounts of $C_{12}E_6$ (~8% mole fraction) caused a slight decrease in the adsorption of CTAB on quartz whereas for roughly equimolar mixtures the total surface excess was close to that of pure $C_{12}E_6$. In a subsequent NR study with oxidised silicon in place of quartz, Penfold *et al.* found that for a 0.1 mM equimolar mixture at pH 7 the adsorbed film was strongly enriched in CTAB compared to the bulk.[7b] Near the isoelectric point of the silica (pH 2.4), mixtures of the two surfactants showed a ~50% increase in

adsorption compared to the pure components.[7a] At low mole fractions of CTAB, the cationic surfactant was enriched in the surface layer while at other concentrations the surface and bulk compositions were approximately equal. Soboleva *et al.* studied the adsorption of a mixture of $C_{14}TAB$ and TX-100 onto quartz sand. They found a small enhancement of the minor component at the surface, but the surface composition was not especially different from the bulk composition.[18]

In this paper we first explore the equilibrium isotherm of CTAB and TX-100 on a planar silica substrate at a total concentration of 2 mM – well above the critical micelle concentration (cmc) of both the pure and mixed systems. This total concentration is used as our benchmark for kinetic measurements. The benchmark compositions were 25%, 50% and 75% CTAB by mole. We also studied the equimolar mixtures at 1 mM and 3 mM concentrations to determine the sensitivity of the adsorption behavior to total surfactant concentration. We report results from five different scenarios: (i) adsorption of mixed surfactant solutions to bare silica, (ii) desorption of mixed surfactant layers into pure water, (iii) displacement of one pure surfactant by another pure surfactant, (iv) displacement of a mixed surfactant layer by a pure surfactant and (v) the displacement of a pure surfactant layer by a mixture.

Our equilibrium measurements on the adsorbed film show strong deviations from ideality and the bulk solution has also been reported to be non-ideal.[19] A quantitative kinetic model, similar to that presented for the pure surfactants in Part I, would require a full characterization of the mixed surfactant system both in the bulk and at the surface at all concentrations and compositions that are encountered during the adsorption or desorption processes. Such a task is a substantial undertaking and we have not attempted it here. The surface measurements alone show a number of unexpected features that can, at a qualitative level, be understood from the non-ideal mixing of the CTAB and TX-100 at the surface.

Experimental

The TIR Raman system has been described in detail in Part I of this work. Briefly, the pump laser is a continuous-wave, frequency-doubled Nd:YAG laser (Opus 532, Laser Quantum, Manchester, UK) with a wavelength of 532 nm. The laser was typically operated at 1.5 W, yielding ~1.0 W at sample. A silica hemisphere was used as the substrate to minimize optical aberrations. The angle of incidence at the silica-water interface was 73.0°, with the beam gently focused to give an illuminated region of 30×10 μm, a penetration depth, d_p for the electric field of 206 nm and a sampling depth for Raman scattering of $d_p/2 = 103$ nm. The incident laser was S polarized (perpendicular to the plane of incidence), since this polarization gave the highest signal levels. The Raman scattered radiation was collected through the fused silica prism with a 50× ULWD, 0.55 NA objective (Olympus) and directed into the spectrometer (Ramascope 1000, Renishaw, Wootton-under-edge, UK). Data were acquired over a fixed wavenumber range encompassing the C–H stretching region (from 2600 to 3200 cm^{-1}) of the Stokes scattering.

For measurements on equilibrium systems, a typical acquisition consisted of ten co-added scans of 30 s each. For the kinetics measurements a much shorter acquisition time of 1 s was used, with a 1s readout time between each measurement limited by the spectrometer software. For ease of comparison, the number of counts on the ordinate is normalized by the acquisition time. A selection of spectra from a kinetic measurement are shown in Figure 1 to provide an indication of spectral quality.
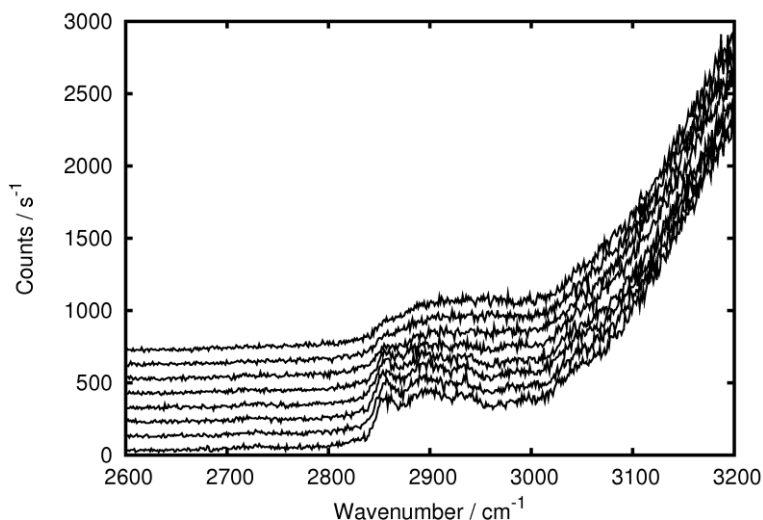
Figure 1: Examples of kinetic spectra, representing *t* = 89–105 s for the system shown later in Figure 11 (b). The spectra are offset on the y-axis for clarity.

Both equilibrium and kinetic measurements were analyzed by a chemometric method known as target factor analysis (TFA).[20] TFA decomposes the dataset into a set of principal components of which the most significant (in this case, arising from water and the two surfactants) are retained and the remainder discarded as noise. These three principal components are actually linear combinations of the Raman spectra of the chemical species present and a coordinate rotation is required to obtain an optimal match to a set of target spectra of the individual chemical species. The result is a refined version of the target spectra and a component weight for each of the target spectra. When multiplied together the component weights and target spectra reproduce the data (without those components discarded as noise). The three target spectra are the spectrum of pure water and the spectra of concentrated solutions of each of the two pure surfactants with the water spectrum manually subtracted (see Figure 2). In the analysis of kinetic data, some spectra from the equilibrium measurements were added to the data set. The greater intensity of the equilibrium spectra compared to kinetics spectra guides the deconvolution of the noisier kinetic spectra towards the known spectra of the individual components. The component weights of the surfactant spectra were scaled by the component weight of the water; scaling compensates for drift in the overall signal level (particularly in equilibrium isotherms that were measured over a full day) and ensures that equilibrium and kinetics measurements are displayed on the same scale. Typically the noise in the each of the individual surfactant components is anti-correlated (see, for example, Figure 6). Therefore, the noise in the total adsorbed amount is less than that of the individual components.

In the isotherms of individual surfactants, the slope of the raw component weight above the cmc can be used to calculate an absolute surface excess, as described in detail in Part I. It is not possible to calibrate the surface excess of a mixture in this way since one cannot assume that the surface excess will remain constant with concentration above the cmc in mixed systems; instead, we determine the surface excess from the strength of the signal relative to the individual pure components. The surface excesses obtained for the individual components are sensitive to the experimental alignment, the spread of angles of incidence and the purity of the surfactants and so should not be taken as exact; the relative magnitude of the surface excess at different concentrations or at different times is accurate, with a precision indicated by the scatter in the data.
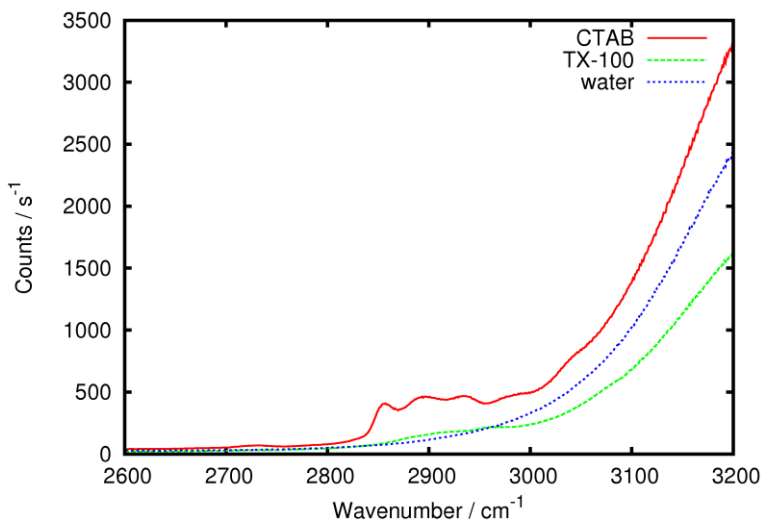
a)
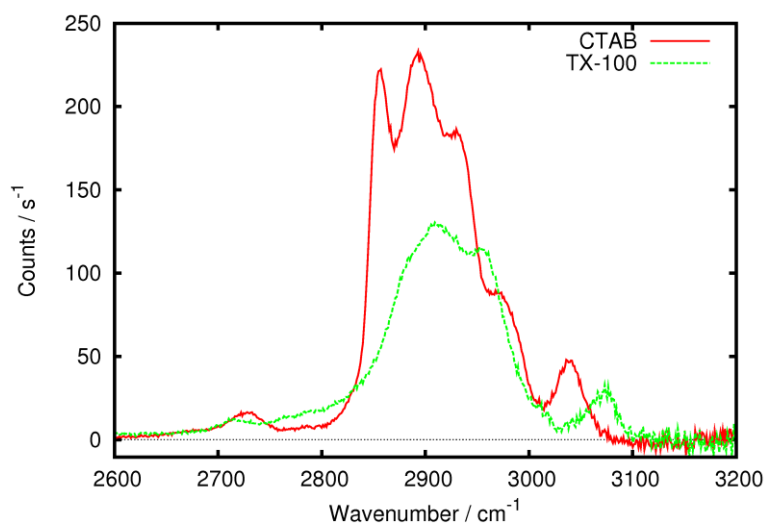
b)

Figure 2: Target spectra for CTAB, TX-100 and water. a) Raw spectra, including target spectrum for water; b) Target spectra for surfactants after subtraction of water background. S polarization. Acquisition time = 360 s.
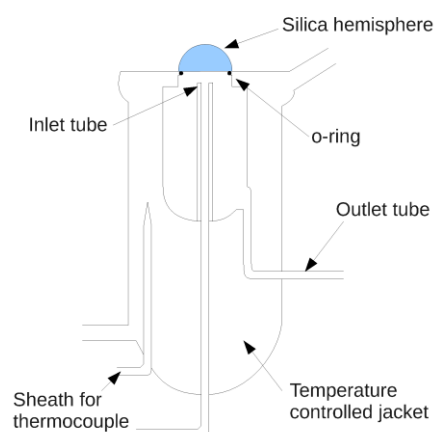
Figure 3: Schematic diagram of the flow cell

All the experiments were conducted using a wall-jet flow cell (Figure 3). The cell has an outer heating jacket connected to a recirculating water bath. All experiments were carried out at 27°C. The inlet tube is 1 mm wide, positioned 1.8 mm below the flat surface of the hemisphere. Solutions were injected at a rate of 0.5 mL min^{-1}. The hydrodynamics of the wall-jet flow cell are well-defined,[21] as discussed in Part I of this work, and allow rapid exchange of the solution in contact with the silica surface.

The cell, tubing and other glassware were cleaned with a commercial alkaline cleaning agent (Borer 15PF concentrate), then rinsed with copious high purity water. The fused silica hemispheres were soaked in chromosulfuric acid for at least 4 h, then rinsed with high purity water. Between each experiment the cell was flushed with at least 100 mL of high purity water to wash any residual surfactant off the surface.

The reproducibility of individual experiments is illustrated by two typical examples in Figure 4. Most of the experimental conditions were repeated at least twice (including all systems that showed non-monotonic behavior), but for clarity only a single example is displayed in the remainder of this paper for each set of conditions.
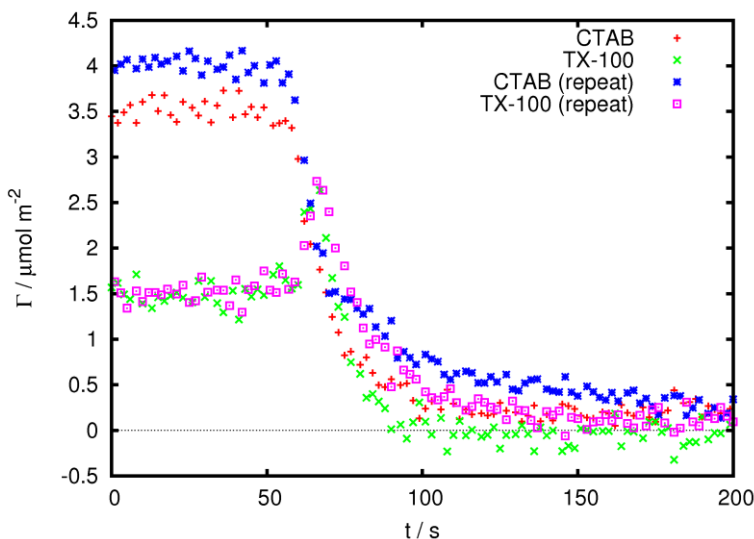
a)
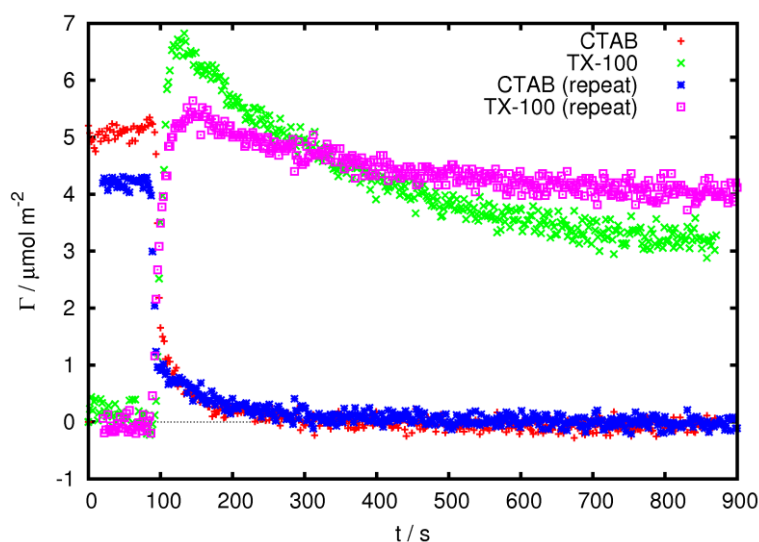
b)

Figure 4: Illustration of the reproducibility of the data for a) a desorption process (shown with explanation in Figure 7 (c)) and b) a replacement process (shown with explanation in Figure 11 (b)).

A complete kinetic model of adsorption and desorption in CTAB/TX-100 mixtures would be a major undertaking of limited generality and which we have not attempted to develop. Nevertheless, it is useful to be able to make some quantitative comparison of the rates of adsorption (or desorption) under different experimental conditions. Consequently, we have evaluated the rates of adsorption or desorption between the points when the change is 30% complete and 70% complete, interpolating linearly between data points to establish these two thresholds where necessary. Some of the adsorption curves display an "overshoot" where the surface excess rises above its equilibrium value; in these cases the change is measured with respect to the highest surface excess. Similarly, some of the desorption processes display a spike before the surface excess begins to fall; when evaluating the rates the change is measured from the top of the spike. Tables showing the maximum rates of flux to and from the surface are given throughout the text. The rate given is a simple average over independent experiments. The variation in the rates observed in repeated experiments on mixtures under nominally identical experimental conditions is typically 20-30% although the

qualitative behavior remains the same. For systems showing the fastest kinetics, the spacing of the data points (every 2 s) limits the accuracy with which the adsorption and desorption rates can be measured.

Results and Discussion

Equilibrium

Part I of this series described the adsorption isotherms for the individual surfactants, CTAB and TX-100, as a function of concentration. Figure 5 presents the surface excess and surface composition for a mixture of CTAB and TX-100 mixture at a constant 2 mM concentration as a function of the mole fraction of CTAB in the mixture.
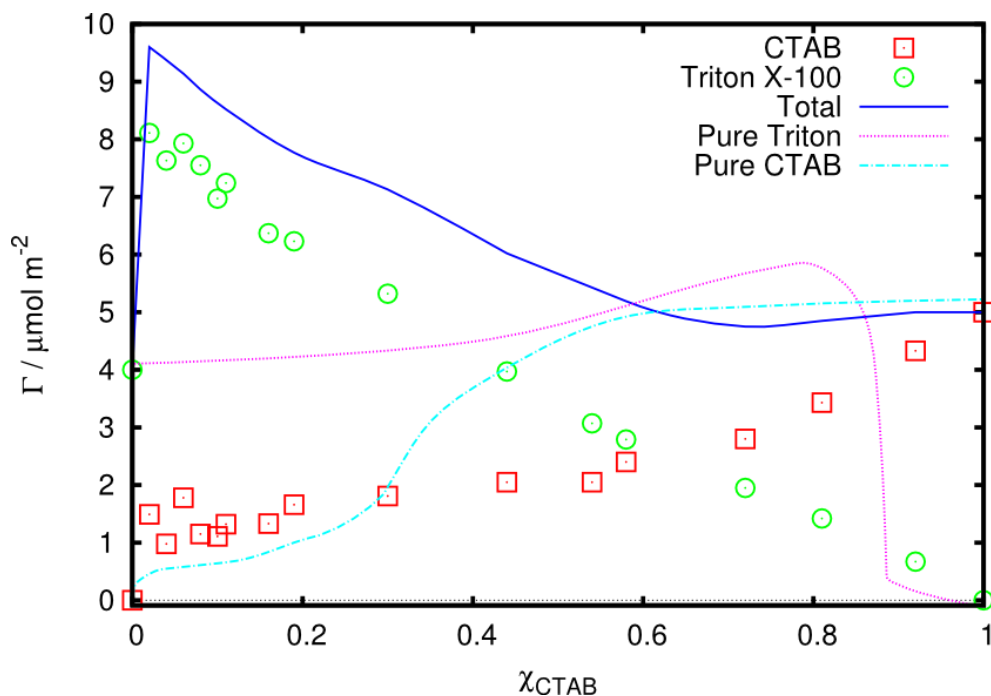
Figure 5: Surface excess of CTAB (squares) and TX-100 (circles) at a total surfactant concentration of 2 mM as a function of the bulk mole fraction of CTAB, χ_{CTAB}, together with the total surface excess (solid line). The isotherms for the pure components at the same concentrations as that component in the mixture are indicated with dotted lines.

The most striking aspect of isotherm in figure 5 is the increase in TX-100 adsorption when tiny amounts of CTAB are added. Even at bulk mole fraction, χ_{CTAB} = 0.02, the TX-100 surface excess was double that of the pure component. The TX-100 surface excess then decreased almost linearly with increasing χ_{CTAB}. In contrast the CTAB surface excess showed a plateau at χ_{CTAB} < 0.6 before rising smoothly as $\chi_{CTAB} \rightarrow$ 1. Consequently, the total adsorbed amount (illustrated by the solid line in Figure 5) is a maximum at very low χ_{CTAB} and then decreases monotonically as the CTAB concentration in the mixture increases.

Figure 5 also the compares the surface excesses in the mixture to those of the pure surfactants at the same bulk concentration. At low χ_{CTAB} there is a synergistic interaction with enhanced adsorption of

both TX-100 and CTAB. For $\chi_{CTAB} > 0.3$, competitive adsorption reduces the surface excess below that of the pure component at the same concentration.

The interactions between CTAB and TX-100 in mixed micelles are known to be favorable,[19] but a favorable interaction parameter alone does not explain the complex adsorption isotherm. The dramatic increase in the total surface excess at low χ_{CTAB} suggests that small amounts of adsorbed CTAB in TX-100-rich layers alters the structure of the surface aggregates to allow more efficient coverage of the surface. Conversely, in CTAB-rich layers, the total surface excess is very similar to that in saturated layer of CTAB, suggesting that the two surfactants are competing for sites within aggregates of a similar structure. Atomic force microscopy might help to identify the nature of adsorbed aggregates, but such measurements are beyond the scope of this work.

Kinetics of adsorption and desorption

We have shown in the Experimental Section that TIR-Raman is able to determine quantitatively the composition of mixed monolayers of CTAB and TX-100 with 1-s acquisition times without the need for deuterated surfactants. Consequently, the rates of adsorption and desorption of the two individual surfactants can be measured separately and not just the rate of change of the total adsorbed amount. Figure 6 shows the adsorption kinetics for a 1:1 mixture at 2 mM total concentration. Both species show a smooth increase in surface coverage with time – the slight overshoot in the TX-100 surface excess is probably a consequence of the polydispersity of the surfactant rather than interactions with the CTAB.

CTAB has a higher cmc than TX-100 (0.9 mM compared with 0.27 mM) so the monomer surfactant is enriched in CTAB compared to the mixture; conversely the micelles are rich in TX-100. Monomers generally diffuse faster than micelles and CTAB diffuses faster than TX-100 (D_{mon} = 8.8 $\times$ 10^{-10} compared with 2.8 $\times$ 10^{-10} $m^2 s^{-1}$), so one might expect CTAB to show faster adsorption kinetics than TX-100. The fact that we observe the reverse shows that adsorption is not under diffusion control.

Table 1 summarizes the adsorption rates (as defined in the Experimental section) for adsorption of various mixtures onto clean silica. The rate of adsorption of TX-100 in mixtures was generally faster than for pure TX-100. One plausible explanation is the favorable hydrophobic interaction of TX-100 with small amounts of CTAB electrostatically bound to the negatively charged silica surface. A second contributing factor may be the increased diffusion coefficient of non-ionic micelles in the presence of a cationic surfactant due to migration fields.
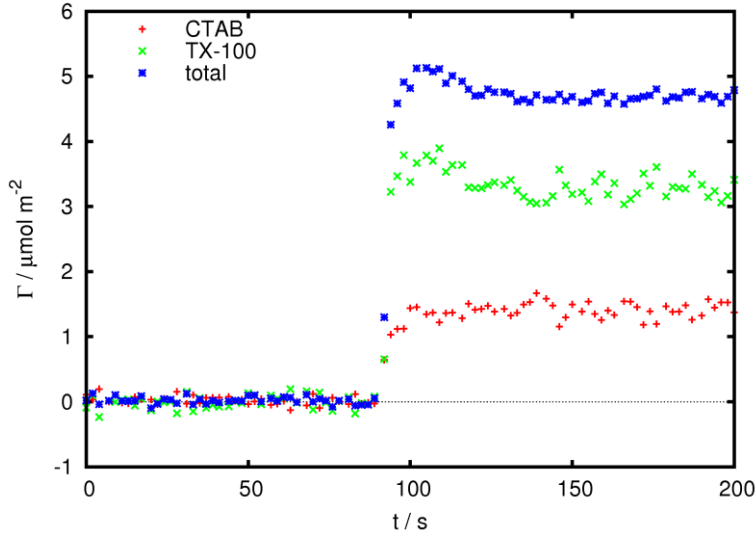
Figure 6: Adsorption of a mixture of CTAB and TX-100 from a 2-mM solution with $\chi_{CTAB} = 0.5$ onto clean silica. Adsorbed amounts: CTAB (+, red), TX-100 (×, green), total (*, blue).

| Total surfactant concentration/ mM	χ_{CTAB}	CTAB rate / μmol m^{-2} s^{-1}	TX-100 rate / μmol m^{-2} s^{-1}
2.0	0.25	0.08	0.6
2.0	0.50	0.10	1.3
2.0	0.75	0.2	0.3
2.0	1	0.7	
2.0	0		0.3
3.0	0.5	0.10	0.7

**Table 1: Rates of adsorption for CTAB/TX-100 mixtures onto a clean silica surface.**

The desorption process is more unusual. Figure 7 shows experimental data for desorption into pure water of surfactant layers adsorbed from surfactant solutions with 2 mM total concentration and $\chi_{CTAB} = 0.25$, 0.5 and 0.75. The CTAB surface excess falls monotonically during the rinsing process but for $\chi_{CTAB} = 0.5$ and 0.75 (Figure 7(b) and (c)) the TX-100 surface excess actually increases sharply at the beginning of the desorption process, peaks after about 10 s and then decays monotonically to zero. In the early part of the desorption process the surface excess remains approximately constant, with desorbing CTAB molecules being replaced by TX-100 adsorbing from the sub-surface layer. For the TX-100-rich system shown in Figure 7(a), the initial surface excess of TX-100 is higher and the peak in the surface excess is less marked; nevertheless, the desorption of TX-100 is delayed compared to CTAB so the surface concentration is enriched in TX-100 during the early part of the desorption process.
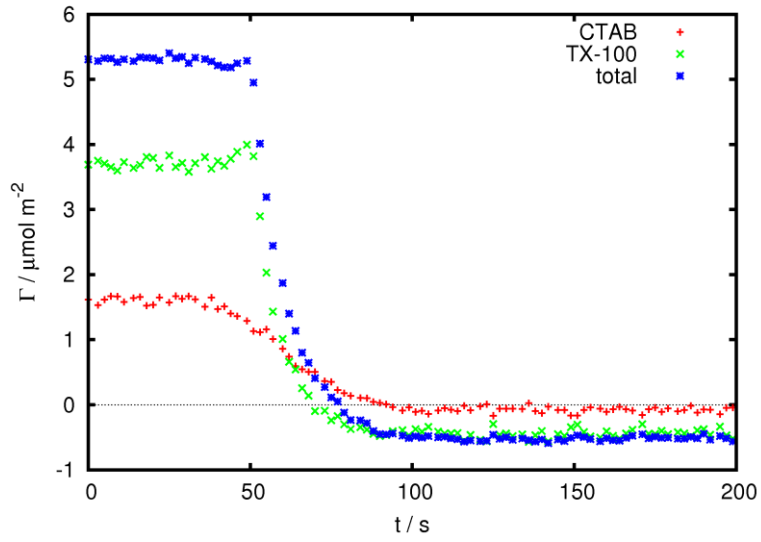
a)
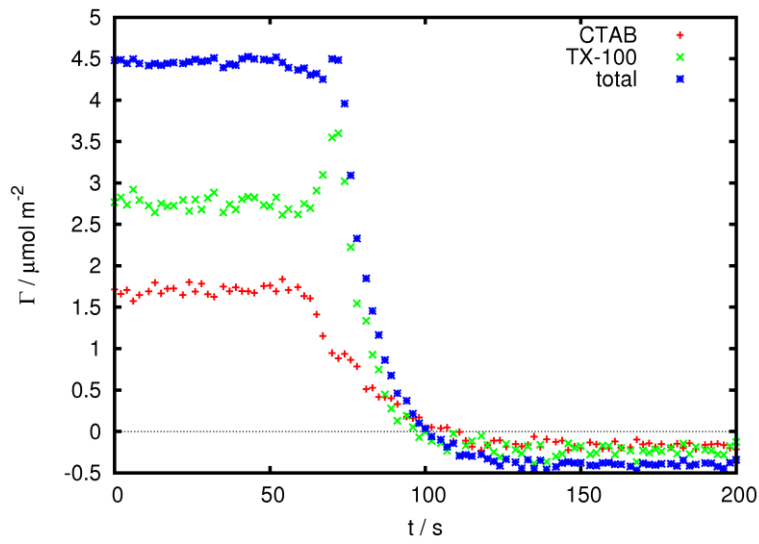
b)
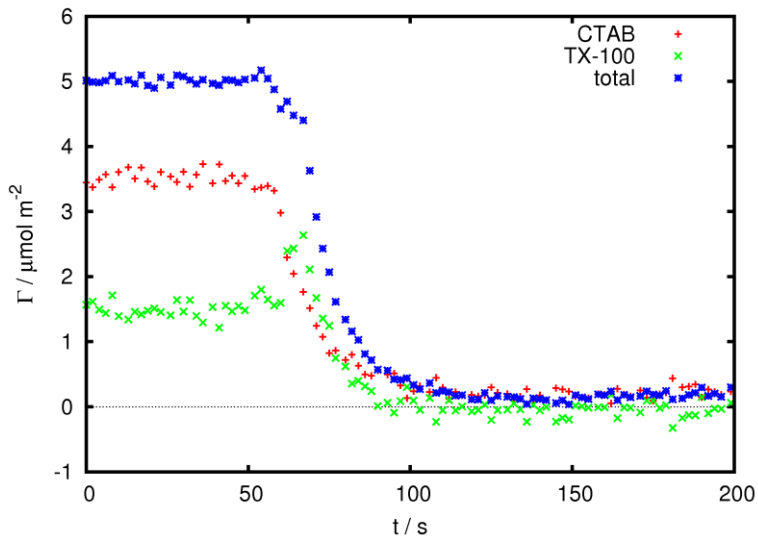
c)

Figure 7: Desorption of mixed layers with an initial solution concentration of 2 mM with χ_{CTAB} = (a) 0.25, (b) 0.5 and (c) 0.75. Pure water was injected into the cell containing the surfactant mixture. Adsorbed amounts: CTAB (+, red), TX-100 (×, green), total (*, blue).

Qualitatively similar behavior was observed for the 3-mM total concentration (Figure 8), though the increase in TX-100 surface excess was less marked than for the 2-mM case.
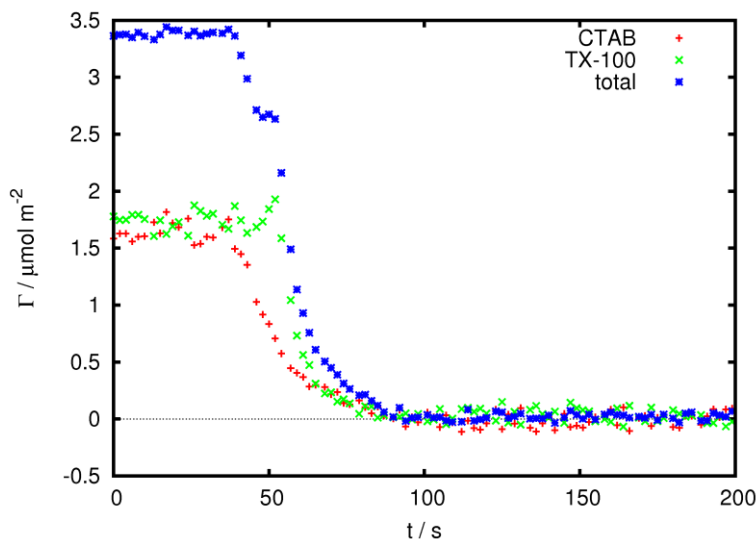

Figure 8: Desorption into pure water of a mixed layers with an initial solution concentration of 3 mM and χ_{CTAB} = 0.5. Adsorbed amounts: CTAB (+, red), TX-100 (×, green), total (*, blue).

This unusual desorption behavior can be understood from the adsorption isotherm (Fig. 5), where a decrease in the surface excess of CTAB leads to a marked increase in the amount of TX-100 adsorbed. The equilibrium mixing behavior is augmented by kinetic factors: CTAB diffuses away from the surface faster than TX-100, for the reasons given earlier, so the local surfactant composition becomes enriched in TX-100 as the total surfactant concentration decreases. So long as the sub-surface concentration remains above the cmc (and assuming the micelles and monomers equilibrate rapidly), an increase in the mole fraction of TX-100 is accompanied by an increase in its chemical potential and hence by an increased driving force to adsorb. Only when the subsurface concentration drops below the cmc, does the chemical potential of the TX-100 begins to fall and the TX-100 desorb from the surface.

A related effect was reported by Brinck *et al.*[10a] for the desorption of mixtures of the non-ionic surfactants $C_{14}E_6$ and $C_{10}E_6$. They found an increase in total surface excess upon desorption though their measurement technique did not permit the determination of the surface excesses of the individual surfactants. They noted that $C_{10}E_6$ is transported away from the surface more rapidly than $C_{14}E_6$ because it has a much higher cmc and thus a higher monomer concentration. As the $C_{10}E_6$ near the surface is depleted, the micelles become enriched in $C_{14}E_6$ and consequently the concentration of monomers of $C_{14}E_6$ in equilibrium with the micelles increases. Since the equilibrium surface excess of $C_{14}E_6$ is higher than for the mixed system, the total adsorbed amount initially increases during the desorption process.

Kinetics of displacement of surfactant layers

The previous section described adsorption onto bare silica or desorption into pure water. Here we consider the displacement of one surfactant layer by a surfactant solution of different composition.

The observed behavior is best classified according to the surfactant being injected, since the results seem to be grouped largely on these lines.

The simplest behavior is seen in systems where pure CTAB replaces an adsorbed layer (either pure TX-100 or a mixture). The replacement of TX-100 by CTAB, both at 2 mM concentration, is shown in Figure 9. The equilibrium isotherm shows that a small amount of CTAB nearly doubles the equilibrium adsorbed amount of TX-100. It is not surprising therefore to observe in Figure 9 that replacement of the TX-100 solution by a CTAB solution initially (though only briefly) increases the adsorbed amount of TX-100. The initial subsurface concentration of TX-100 is 7 times the cmc, so one might expect a significant delay before TX-100 desorbed from the surface. The CTAB diffusing towards the surface, however, forms mixed micelles with the TX-100 which immediately lowers the chemical potential of the TX-100, driving desorption into solution. The initial rate of adsorption of CTAB to a TX-100 covered surface is initially similar to that on bare silica (Figure 9 and Table 2) – a surprising result from the Langmuir perspective that would predict an adsorption rate proportional to the fraction of unfilled sites $(1-\theta)$. From the Frumkin perspective, however, the $(1-\theta)$ reduction is offset by an increase in the adsorption rate constant $k_a e^{\omega_a \Gamma / \Gamma_\infty}$ (see Part I) owing to attractive interactions between hydrocarbon chains: it appears that these two effects are roughly in balance. Once the surface concentration of CTAB reaches that of TX-100, the rates of adsorption of CTAB and desorption of TX-100 both decrease markedly. In particular, desorption of TX-100 into a CTAB solution is an order of magnitude slower than into pure water (see Part I, fig. 16). This reduction in rate can be ascribed, at least in part, to the interactions between the two surfactants, which favor a mixed layer relative to a pure layer of either surfactant.
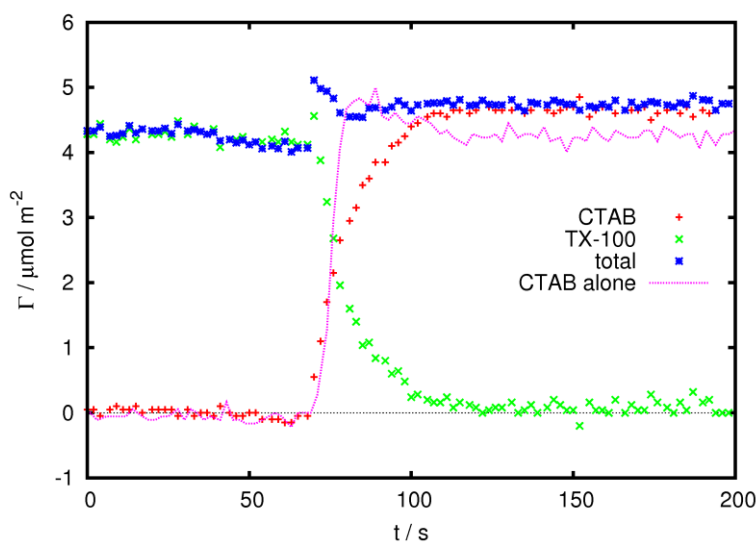

Figure 9: Replacement of 2 mM TX-100 (green ×) with 2 mM CTAB (red +). The total surface excess is shown as blue stars. The adsorption of 2 mM CTAB onto a clean silica surface (line) is shown for comparison.

For the case when CTAB replaces a mixed layer, there is no transient increase in the TX-100 concentration, but only a smooth replacement of TX-100 by CTAB. The qualitative behavior is insensitive to either concentration or composition. An illustrative example in which a 1:1 mixture of TX-100 and CTAB is replaced by pure CTAB is shown in Figure 10. The total adsorbed amount

remains approximately constant during the displacement process (the surface remains fully covered with surfactant) and consequently the adsorption and desorption rates are nearly equal (see Table 2). The rates of exchange of CTAB for TX-100 are typically a factor of 5 slower than for adsorption of CTAB to a bare surface or desorption of TX-100 into water. We note that only a chemically selective technique such as TIR-Raman can reveal the kinetics of exchange in this system.

Concentration / mM	System being replaced	χ_{CTAB}	System being injected	CTAB rate / μmol m^{-2} s^{-1}	TX-100 rate / μmol m^{-2} s^{-1}
1	TX-100	—	CTAB	0.14	–0.19
2	TX-100	—	CTAB	0.17	–0.20
3	TX-100	—	CTAB	0.23	–0.14
1	mixture	0.5	CTAB	0.09	–0.06
2	mixture	0.25	CTAB	0.14	–0.18
2	mixture	0.5	CTAB	0.18	–0.21
2	mixture	0.75	CTAB	0.10	–0.05
3	mixture	0.5	CTAB	0.15	–0.10
2	Water	—	CTAB	0.7	
2	TX-100	—	Water		–1.1

Table 2: Rates of replacement of TX-100 or mixtures of TX-100 and CTAB with an equal concentration of CTAB. Comparative rates for the pure surfactant systems are also shown. Negative numbers indicate desorption.
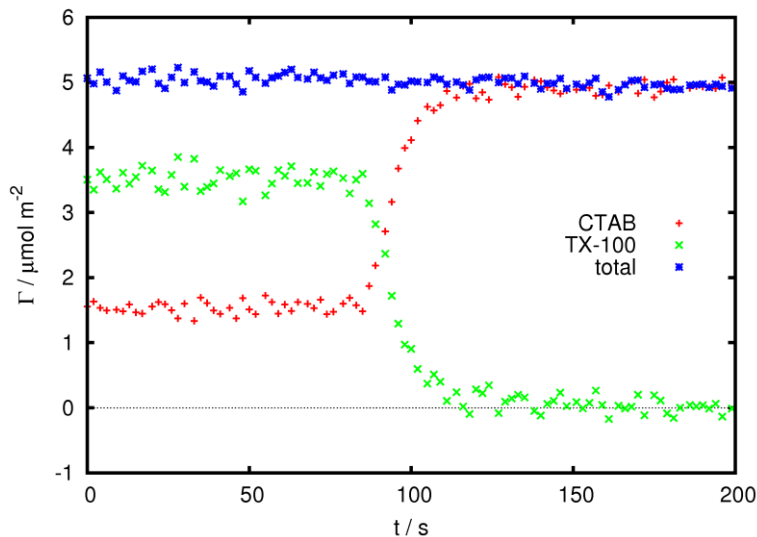

Figure 10: Injection of a 2-mM solution of CTAB into a 2-mM surfactant mixture with χ_{CTAB} = 0.5. Adsorbed amounts: CTAB (+, red), TX-100 (×, green), total (*, blue).

The reverse situation, in which TX-100 replaces an adsorbed layer of CTAB, shows quite unusual behavior. Figure 11 shows the kinetic traces when the initial CTAB concentration and final TX-100 concentration are 1 mM, 2 mM or 3 mM. At first glance the curves seem to show extreme concentration dependence, but closer inspection shows that in all cases the total concentration (blue stars in Figure 11) first drops sharply (though only for 2 s in the 2-mM example) then increases steeply – overshooting the equilibrium adsorbed amount – and finally decays slowly to equilibrium. Variations in the relative timing of the desorption and adsorption (arising from the complex dependence of the mass transport rates and monomer concentrations on the total concentration of surfactant as well as the composition) determine how pronounced is the dip in total coverage at short times.
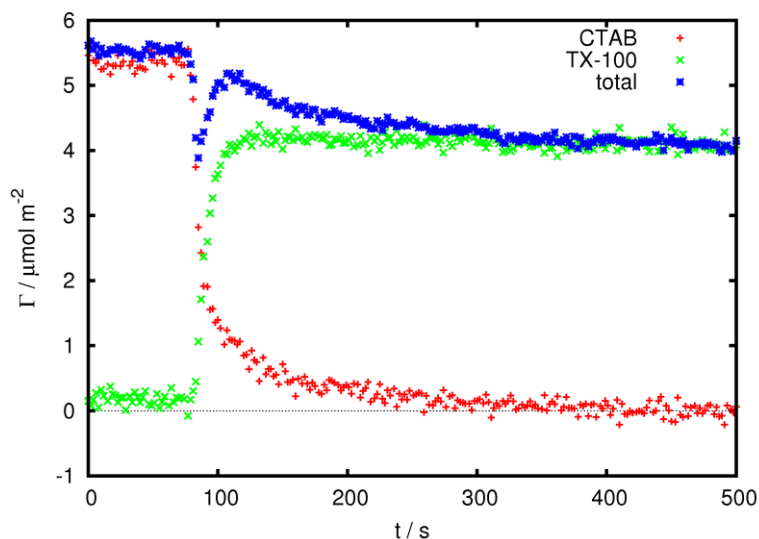
a)
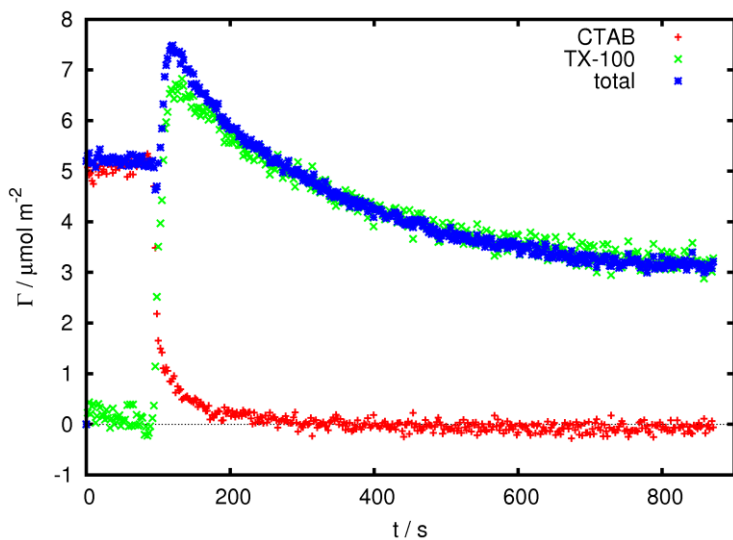
b)
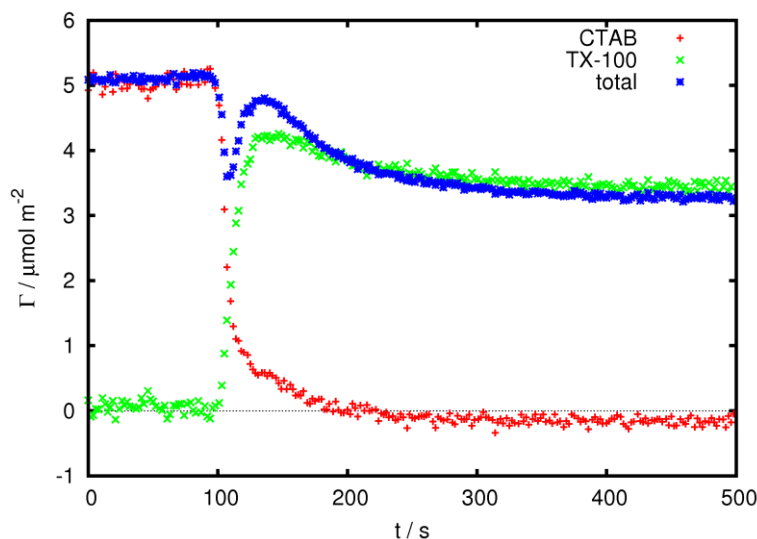
c)

Figure 11: Replacement of CTAB (red +) by TX-100 (green ×) at a) 1 mM, b) 2 mM and c) 3 mM concentrations. The total surface excess is shown as blue stars. Note that temporal axis in b) is different from a) and c), because of the longer time required for the surface to reach equilibrium.

Turning to the individual components, the CTAB desorption is similar in all three plots – a steep initial decline followed by a long tail reflecting the plateau in the CTAB adsorption isotherm at low concentrations (Figure 5). The TX-100 concentration profiles at 2 mM and 3 mM (Figure 11(b) and (c)) overshoot the final surface excesses before slowly relaxing to equilibrium. This overshoot is most pronounced in the 2 mM case and it takes more than ten minutes for equilibrium to be reached. The overshoot in the adsorption of the non-ionic surfactant can be understood from the equilibrium isotherm in Figure 5: the incorporation of even a trace of CTAB in the adsorbed layer greatly increases the surface excess of TX-100. Not until the last remnants of CTAB are rinsed from the surface does the TX-100 reach its final coverage. For reasons that are not clear, the 1-mM concentration, while still showing a slow approach to equilibrium, does not show an overshoot in the TX-100 concentration.

A related set of experiments is the replacement of mixtures of different compositions by pure TX-100. The observed kinetics are similar to the replacement of pure CTAB with TX-100, only starting from a later time where the surface is already of mixed composition. For this reason, the dip in the total adsorbed amount, which occurs in Figure 11 at low surface excesses of TX-100, is not observed when the starting film already contains a significant amount of TX-100. An example of the displacement of a 2 mM equimolar solution with pure TX-100 is shown in figure 12. The measured rates are tabulated in Table 3; they are slower than for the replacement of CTAB by TX-100, especially the rate of desorption. This difference is expected, since the fast initial changes seen in Figure 11 are bypassed in the mixed initial solutions. CTAB shows a long tail in its desorption, and the processes for mixed systems are starting from a point that is near the start of that tail.

Concentration / mM	System being replaced	χ_{CTAB}	System being injected	CTAB rate / μmol m^{-2} s^{-1}	TX-100 rate / μmol m^{-2} s^{-1}
1	CTAB	—	TX-100	-0.21	0.21
2	CTAB	—	TX-100	-0.27	0.30
3	CTAB	—	TX-100	-0.28	0.21
1	mixture	0.5	TX-100	-0.04	0.12
2	mixture	0.25	TX-100	-0.026	0.09
2	mixture	0.5	TX-100	-0.030	0.19
2	mixture	0.75	TX-100	-0.042	0.23
3	mixture	0.5	TX-100	-0.04	0.10
2	Water	—	TX-100		0.34
2	CTAB	—	Water	-0.39	

Table 3: Rates of adsorption of TX-100 and desorption of CTAB for replacement of either CTAB or a mixed layer by TX-100. Equivalent rates for the individual systems adsorbing and desorbing are shown for comparison.
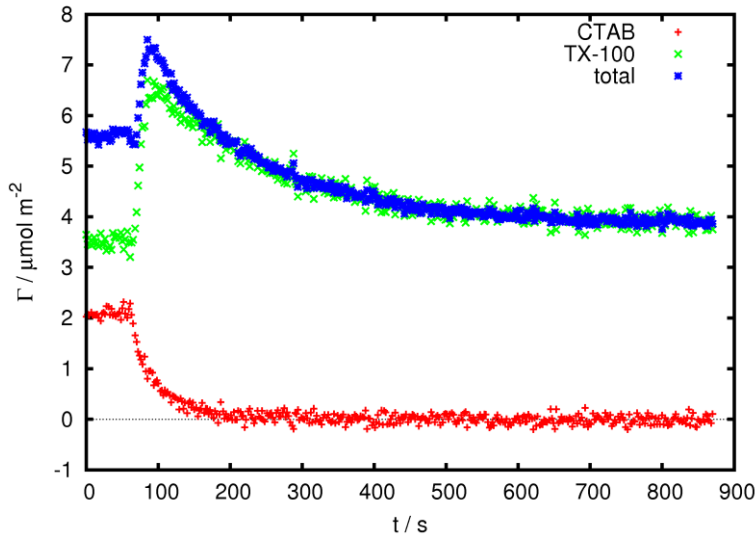

Figure 12: Replacement of a 2-mM mixed surfactant solution with χ_{CTAB} = 0.5 by 2-mM TX-100. Adsorbed amounts: CTAB (+, red), TX-100 (×, green), total (*, blue).

The final permutation on displacement kinetics involves the replacement of a single surfactant by a variety of different mixed surfactant solutions. There are two variations within this category depending on whether the initial layer is composed of CTAB or TX-100.

Where mixtures replace CTAB the results are largely unremarkable: the exchange of components at the surface happens at a rate largely similar to that seen for replacement by pure surfactants (rates

are tabulated in table 4). The rates of CTAB desorption are generally greater than the rates of TX-100 adsorption. In some cases this disparity in rate leads to a temporary drop in total surface excess as the exchange proceeds. An example is shown in figure 13(b) for replacement of a 2-mM CTAB solution by a 2-mM mixture with $\chi_{CTAB} = 0.5$.
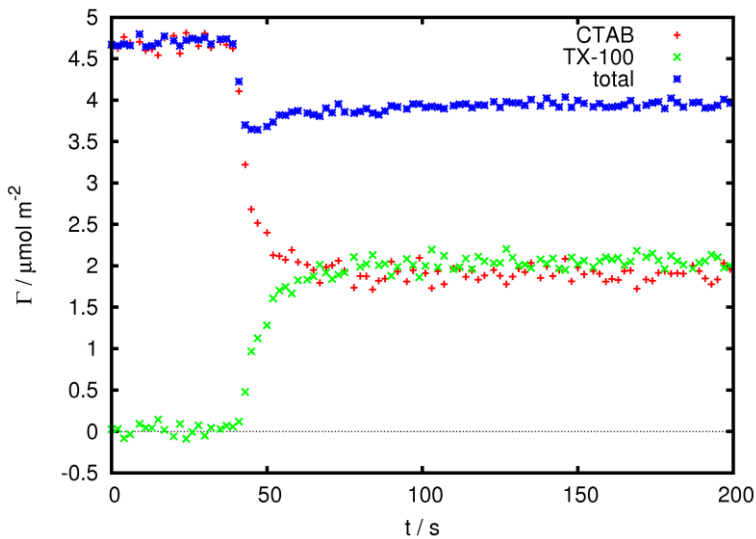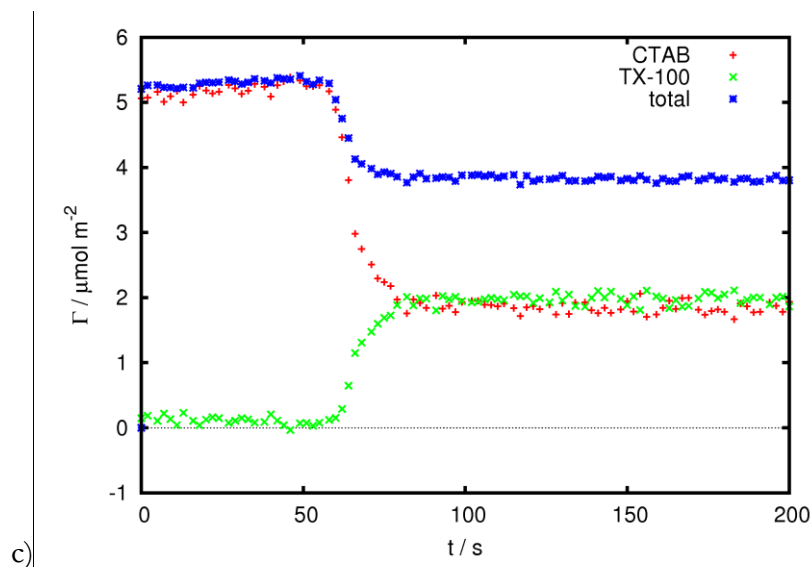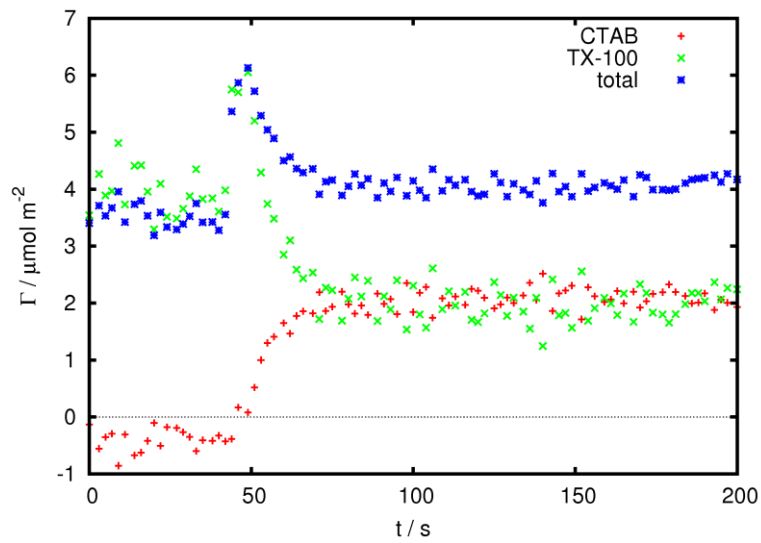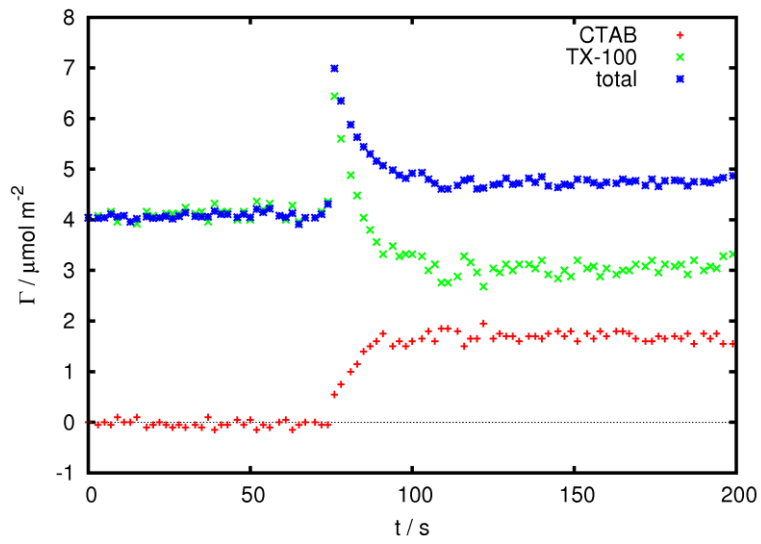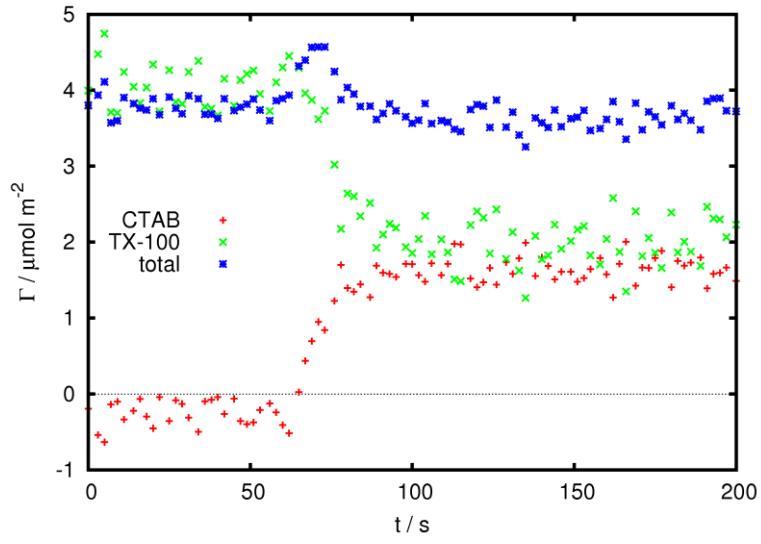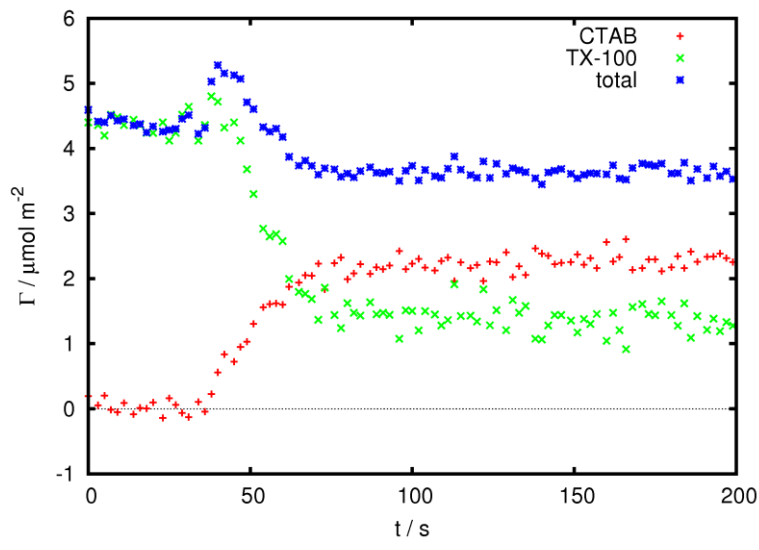

a)
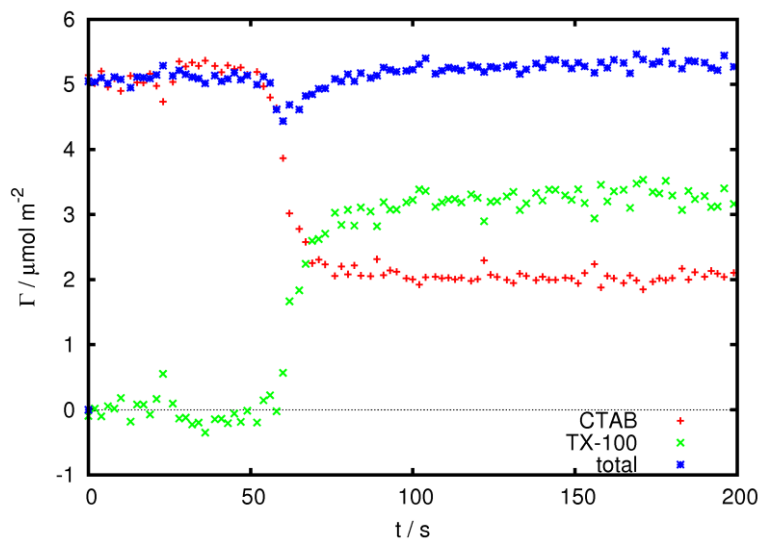
b)

Figure 13: Replacement of a CTAB solution with a surfactant mixture at the same total concentration with χ_CTAB = 0.5. (a) 1 mM, (b) 2 mM and (c) 3 mM. Adsorbed amounts: CTAB (+, red), TX-100 (×, green), total (*, blue).

The most interesting interfacial behavior seems to arise when TX-100 is mixed with just a small amount of CTAB at the surface. We would therefore expect that the replacement of TX-100 by a mixture containing CTAB would result in a sharp increase in the adsorbed amount and this is indeed observed. Figure 14(b) shows the replacement of a 2 mM TX-100 solution by a 2 mM mixture with χ_{CTAB} = 0.5. This experiment is the reverse of the experiment shown in Figure 10. The TX-100 coverage shows a sharp spike as the first CTAB adsorbs to the surface. Since the local concentration of TX-100 is still close to 2 mM, this adsorption occurs very rapidly – too rapidly for us to resolve with the current spectrometer. The TX-100 adsorption then decreases quickly towards its equilibrium value as more CTAB competes for space in the adsorbed layer. The total adsorbed amount shows a similar transient spike. Figure 14(c) shows the equivalent experiment with 2.5 mM solutions, and shows similar results as for 2 mM.

In the case of TX-100 replacing CTAB (Figure 11), we noted the absence of an overshoot in the TX-100 excess for the lower concentration of 1 mM. This behavior is repeated here. Figure 14(a) shows the replacement of 1 mM TX-100 by an equimolar surfactant mixture: there is a smooth replacement of TX-100 by CTAB with almost no change in the total surface excess. Two higher concentrations were also studied. A 3 mM sample (Figure 14(d)) showed only a small spike in TX-100 surface excess, compared with 2 mM and 2.5 mM samples, but a pronounced spike re-emerges at 10 mM concentration (Figure 14(e)). The maximum adsorption and desorption rates are tabulated in table 4.

a)

b)

c)

d)
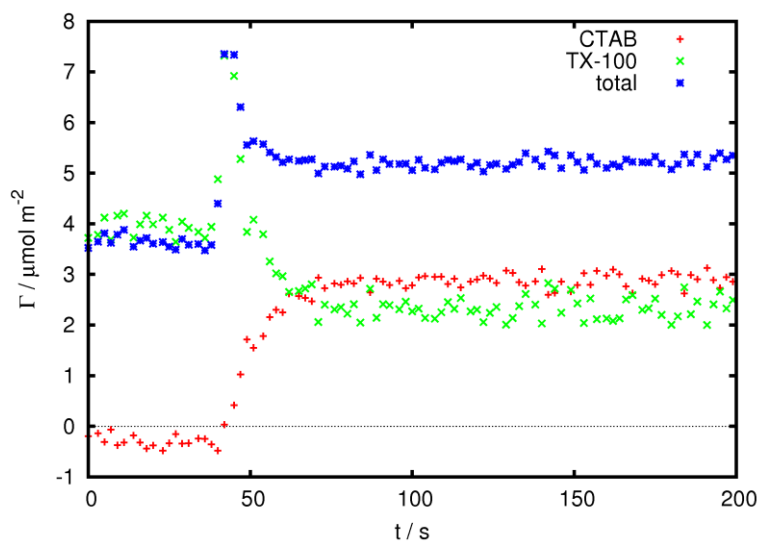
e)

Figure 14: Replacement of a TX-100 solution with a surfactant mixture at the same total concentration with χ_{CTAB} = 0.5. a) 1 mM, b) 2 mM, c) 2.5 mM, d) 3 mM and e) 10 mM total concentration. Adsorbed amounts: CTAB (+, red), TX-100 (×, green), total (*, blue).

System replaced	Concentration / mM	System injected χ_{CTAB}	CTAB rate / μmol m^{-2} s^{-1}	TX-100 rate / μmol m^{-2} s^{-1}
CTAB	1	0.5	-0.36	0.12
CTAB	2	0.25	-0.38	0.23
CTAB	2	0.5	-0.27	0.17
CTAB	2	0.75	-0.13	0.06
CTAB	3	0.5	-0.29	0.12
TX-100	1	0.5	0.07	-0.09
TX-100	2	0.25	0.034	-0.11
TX-100	2	0.5	0.10	-0.19
TX-100	2	0.75	0.09	-0.18
TX-100	2.5	0.5	0.11	-0.14
TX-100	3	0.5	0.07	-0.13
TX-100	10	0.5	0.15	-0.25

Table 4: Rates of adsorption and desorption when mixed solutions replace a single surfactant solution.

Conclusions

The first objective of this work was to demonstrate that total internal reflection Raman scattering can be used to study the adsorption kinetics of surfactant mixtures with chemical selectivity. We have shown for the system CTAB + TX-100 that interfacial kinetics can be followed with 2-s time resolution and a typical precision of $< 2 \times 10^{-7}$ mol m^{-2} in the adsorbed amount of each component. The spectrometer is not optimized for fast kinetics and technical improvements such as a back-thinned CCD and customized software would improve the time resolution to 0.5 s. This time resolution is still inferior to that achievable by non-chemically selective techniques such as ellipsometry,[10] but is sufficiently fast to follow almost all the adsorption, desorption and displacement experiments presented in this paper.

Chemometric methods for data analysis are an indispensable aid for processing sets of kinetic spectra and allowed us to distinguish CTAB and TX-100 without selective deuteration of one component. Principal component analysis proved successful even for strongly overlapping spectra, but the surfactant spectra do need to have some distinguishing features. For example, the two surfactants in the study be Brinck and co-workers[10] discussed earlier — $C_{10}E_6$ and $C_{14}E_6$ — could not be distinguished by TIR-Raman without deuteration of one component. TIR-Raman is not restricted to silica as a substrate: in work to be presented elsewhere we will show that the silica can be coated with a thin organic film and the kinetics of adsorption of surfactant mixtures to the organic surface can still be extracted from the Raman spectra.

CTAB and TX-100 mix non-ideally both in the bulk and at a surface. Although there is no direct interaction between the hydrophobic chains or between the head groups leading to a favorable

interaction parameter, the presence of the non-ionic surfactant between cationic surfactants reduces the electrostatic repulsions from the charged head groups while the relatively small trimethyl ammonium head group reduces the steric repulsions between the polymer-like polyethylene oxide chains of the non-ionic surfactant. At a hydrophilic silica surface, the adsorption isotherms of the two surfactants are qualitatively different: while both show a step in the isotherm at a concentration just below the bulk cmc, CTAB shows a plateau in the adsorption isotherm at lower concentrations while TX-100 shows no adsorption. Small amounts of CTAB bound electrostatically to the silica have a dramatic effect on the adsorption isotherm of TX-100. In a 2-mM solution of TX-100, the equilibrium amount of adsorbed TX-100 doubled in the presence of only 2% mole fraction CTAB. These interactions also have a major influence on the interfacial kinetics. When solutions containing CTAB are replaced with pure TX-100, the surface excess of TX-100 overshoots its equilibrium value and only relaxes to that of the pure system after all the CTAB has been washed away from the surface. Similarly, when replacing pure TX-100 with a mixed system the first CTAB to reach the surface induces a sharp rise in TX-100 adsorption. Mass transport effects also produce interesting behavior. During rinsing of mixed surfactant layers with pure water, the more rapid transport of CTAB away from the surface causes a temporary increase in TX-100 monomer concentration in the subsurface region, which in turn leads to a brief spike in the TX-100 surface excess before the main desorption process commences.

References

1.	(a) Vollhardt, D.; Czichocki, G., *Langmuir* **1990,** *6* (2), 317-322; (b) Lu, J. R.; Purcell, I. P.; Lee, E. M.; Simister, E. A.; Thomas, R. K.; Rennie, A. R.; Penfold, J., *Journal of Colloid and Interface Science* **1995,** *174* (2), 441-455.

2.	Rosen, M. J., *Surfactants and Interfacial Phenomena*. 3rd ed.; John Wiley & Sons, Inc.: Hoboken, New Jersey, 2004.

3.	Quintero, L., *Journal of Dispersion Science and Technology* **2002,** *23* (1), 393 - 404.

4.	A. Bos, M.; van Vliet, T., *Advances in Colloid and Interface Science* **2001,** *91* (3), 437-471.

5.	Briscoe, W. H.; Titmuss, S.; Tiberg, F.; Thomas, R. K.; McGillivray, D. J.; Klein, J., *Nature* **2006,** *444* (7116), 191-194.

6.	(a) Partyka, S.; Zaini, S.; Lindheimer, M.; Brun, B., *Colloids and Surfaces* **1984,** *12*, 255-270; (b) Paria, S.; Manohar, C.; Khilar, K. C., *Industrial & Engineering Chemistry Research* **2005,** *44* (9), 3091-3098; (c) Biswas, S. C.; Chattoraj, D. K., *Journal of Colloid and Interface Science* **1998,** *205* (1), 12-20.

7.	(a) Penfold, J.; Staples, E. J.; Tucker, I.; Thomas, R. K., *Langmuir* **2000,** *16* (23), 8879-8883; (b) Penfold, J.; Staples, E. J.; Tucker, I.; Thompson, L. J., *Langmuir* **1997,** *13* (25), 6638-6643.

8.	Velegol, S. B.; Tilton, R. D., *Langmuir* **2000,** *17* (1), 219-227.

9.	Postmus, B. R.; Leermakers, F. A. M.; Koopal, L. K.; Cohen Stuart, M. A., *Langmuir* **2007,** *23* (10), 5532-5540.

10.	(a) Brinck, J.; Jönsson, B.; Tiberg, F., *Langmuir* **1998,** *14* (20), 5863-5876; (b) Brinck, J.; Tiberg, F., *Langmuir* **1996,** *12* (21), 5042-5047.

11.	Couzis, A.; Gulari, E., Adsorption from Aqueous Binary Surfactant Mixtures onto the Solid-Liquid Interface. In *Mixed Surfactant Systems*, American Chemical Society: 1992; Vol. 501, pp 354-365.

12.	Clark, S. C.; Ducker, W. A., *The Journal of Physical Chemistry B* **2003,** *107* (34), 9011-9021.

13.	Li, H.; Tripp, C. P., *The Journal of Physical Chemistry B* **2004,** *108* (47), 18318-18326.

14.	Tabor, R. F.; Eastoe, J.; Dowding, P., *Langmuir* **2009,** *25* (17), 9785-9791.

15.	Day, J. P. R.; Campbell, R. A.; Russell, O. P.; Bain, C. D., *The Journal of Physical Chemistry C* **2007,** *111* (25), 8757-8774.

16.	Huang, Z.; Gu, T., *Colloids and Surfaces* **1987,** *28*, 159-168.

17.	McDermott, D. C.; Kanelleas, D.; Thomas, R. K.; Rennie, A. R.; Satija, S. K.; Majkrzak, C. F., *Langmuir* **1993,** *9* (9), 2404-2407.

18.	Soboleva, O. A.; Yaroslavtsev, A. A.; Badun, G. A.; Summ, B. D., *Colloid Journal* **2004,** *66* (4), 470-476.

19.   Carnero Ruiz, C.; Aguiar, J., *Molecular Physics: An International Journal at the Interface Between Chemistry and Physics* **1999,** *97* (10), 1095 - 1103.

20.   Malinowski, E. R., *Factor Analysis in Chemistry*. 2nd ed.; John Wiley & Sons, Inc.: 1991.

21.   Dabroś, T.; van de Ven, T. G. M., *Colloid & Polymer Science* **1983,** *261* (8), 694-707.